Journal of Hazardous Materials 460 (2023) 132486

Contents lists available at ScienceDirect

Journal of Hazardous Materials

journal homepage: www.elsevier.com/locate/jhazmat

Sulfate-reduction and methanogenesis are coupled to Hg(II) and MeHg reduction in rice paddies

Qingqing Wu [a,b], Baolin Wang [a], Haiyan Hu [a,*], Andrea G. Bravo [c], Kevin Bishop [d], Stefan Bertilsson [d], Bo Meng [a], Hua Zhang [a,*], Xinbin Feng [a,b]

[a] State Key Laboratory of Environmental Geochemistry, Institute of Geochemistry, Chinese Academy of Sciences, Guiyang 550081, China
[b] University of Chinese Academy of Sciences, Beijing 100049, China
[c] Department of Marine Biology and Oceanography, Institut de Ciencies del Mar (ICM-CSIC), Barcelona E08003, Catalunya, Spain
[d] Department of Aquatic Sciences and Assessment, Swedish University of Agricultural Sciences, Uppsala SE-75007, Sweden

HIGHLIGHTS

- Sulfate-reduction intensely affected Hg (II) reduction in highly Hg-contaminated paddy soils.
- Methanogenesis is an important microbial process controlling MeHg reduction in rice paddies.
- Oxidative demethylation is the dominant pathway of MeHg demethylation in rice paddy soils.
- Hg(II) reduction may constrain Hg(II) methylation in rice paddy soil at the abandoned Hg mining site.

GRAPHICAL ABSTRACT

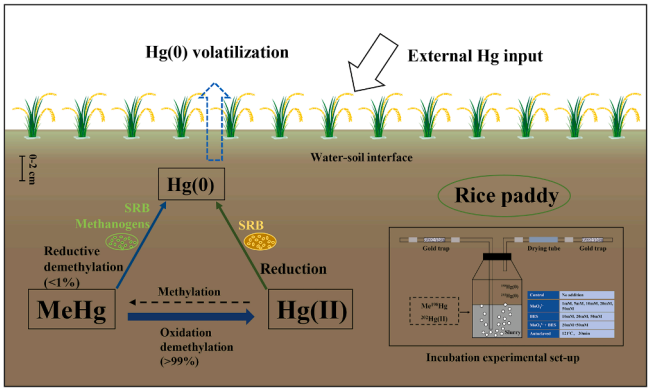

ARTICLE INFO

Editor: Jörg Rinklebe

Keywords:
Mercury reduction
Demethylation
Biogeochemical cycle
Microbial metabolism
Rice paddy

ABSTRACT

Methylmercury (MeHg) produced in rice paddies is the main source of MeHg accumulation in rice, resulting in high risk of MeHg exposure to humans and wildlife. Net MeHg production is affected by Hg(II) reduction and MeHg demethylation, but it remains unclear to what extent these processes influence net MeHg production, as well as the role of the microbial guilds involved. We used isotopically labeled Hg species and specific microbial inhibitors in microcosm experiments to simultaneously investigate the rates of Hg(II) and MeHg transformations, as well as the key microbial guilds controlling these processes. Results showed that Hg(II) and MeHg reduction rate constants significantly decreased with addition of molybdate or BES, which inhibit sulfate-reduction and methanogenesis, respectively. This suggests that both sulfate-reduction and methanogenesis are important processes controlling Hg(II) and MeHg reduction in rice paddies. Meanwhile, up to 99% of MeHg demethylation was oxidative demethylation (OD) under the incubation conditions, suggesting that OD was the main MeHg degradative pathway in rice paddies. In addition, [^{202}Hg(0)/Me^{202}Hg] from the added $^{202}Hg(NO_3)_2$ was up to 13.9%, suggesting that Hg(II) reduction may constrain Hg(II) methylation in rice paddies at the abandoned Hg

* Corresponding authors.
E-mail addresses: huhaiyan@mail.gyig.ac.cn (H. Hu), zhanghua@mail.gyig.ac.cn (H. Zhang).

https://doi.org/10.1016/j.jhazmat.2023.132486
Received 14 June 2023; Received in revised form 17 August 2023; Accepted 3 September 2023
Available online 9 September 2023

mining site. This study improves our understanding of Hg cycling pathways in rice paddies, and more specifically how reduction processes affect net MeHg production and related microbial metabolisms.

1. Introduction

Mercury (Hg) is a global pollutant with methylmercury (MeHg) as the most harmful species which is prone to both bioaccumulation and biomagnification in food webs [1,2]. Hg contaminated rice has been reported in many countries and regions around the world [3–5] and public concerns about health risks associated with rice consumption has risen in recent years [6,7]. Historical Hg mining activities have resulted in high Hg contamination levels in soil, water and air within the areas surrounding mining operations [8]. Rice grain with high MeHg concentration ($\geq$100 $\mu g \cdot kg^{-1}$) has for example been found in the Wanshan area, Guizhou province, southwestern China, where Hg has been mined for thousands of years [9]. Paddy fields are known to be "hotspots" for MeHg production due to the favorable conditions for Hg(II) methylation created by flooding during the rice growing season. These land management strategies result in accumulation of MeHg in rice plants and subsequently also in rice grain [7,10,11]. The MeHg accumulation in rice grain is controlled by net MeHg production in paddy soils, which was greatly affected by microbial activities of methylators [12,13], and many environmental factors, such as soil pH [14], redox (Eh) [15–17], and organic matter (OM) [18,19].

Hg(II) methylation is mediated by various lineages of anaerobic microorganisms that host *hgcAB* genes. This includes metabolic guilds such as sulfate reducing bacteria (SRB), iron-reducing bacteria (FeRB), methanogens and fermenters [20,21]. Hg(II) methylation is controlled by (1) the amount of Hg and more specifically the bioavailable Hg(II), constrained by Hg(II) speciation [22–27] and microbial processes, such as Hg(II) reduction which may deplete the pool of bioavailable Hg(II), or oxidation that replenish the pool of Hg(II) available to methylators [28]; (2) the activity of Hg methylating microorganisms [29–31]. Significant progress has been made since the Hg research community became aware of health hazards related to MeHg exposure via rice consumption. For instance, we have a better understanding of the rice paddy microbial communities involved in Hg(II) methylation [12,32–35]. However, in these earlier studies, the impact of Hg(II) reduction and MeHg demethylation on MeHg production have been largely overlooked.

Net MeHg production is determined by two competing processes, Hg(II) methylation and MeHg demethylation [36]. MeHg demethylation can be mediated by both biotic and abiotic processes [35,37] while methylation is mainly a biological process. MeHg degradation is to occur via two alternative pathways [37]. Reductive demethylation (RD) is enabled by the *mer* operon and produces CH_4 and Hg(0). This mainly occurs under oxic conditions at relatively high Hg concentrations [37–41]; Oxidative demethylation (OD), analogous to methylation, is mediated by anaerobic microorganisms at relatively low Hg concentrations and produces CO_2 and Hg(II) [37]. RD results in net removal of Hg as Hg(0) is volatile [37,42], while OD, yielding Hg(II), may promote the methylation-demethylation cycle [43]. Besides biotic reduction, Hg(II) can also be reduced to Hg(0) by abiotic processes, e.g. via electron transfer from OM and FeS minerals in the absence of oxygen [44–46]. It has been reported that the most significant microbial reduction in sediment occurred in anaerobic dark layers [47–49]. However, it is still unclear which demethylation pathway is dominant in rice paddy soils.

Microorganisms are one of the vital factors affecting the biogeochemical cycling of Hg in the environment. Due to the complexity of the rice paddy soil environment, researchers usually study the microbial impacts on Hg transformation as correlations between Hg dynamics, environmental factors and soil microbial communities. Potential methylating/demethylating lineages have been identified [33,35], and sulfate-reducing δ-Proteobacteria and methanogenic Archaea have positively correlated with MeHg and THg concentrations in Hg-contaminated rice paddy soils [34]. Hg(0) is a common Hg species in nature, and it is readily formed in both soil and aquatic environments. Less is known about Hg reduction in paddy soil, even if Hg reduction could result in a significant decrease in the amount of Hg available for methylation. Hg(II) reduction is furthermore the primary Hg-detoxifying mechanism used by Hg-resistant bacteria [50]. Excessive Hg concentrations can induce phenotypic responses in some bacteria, such as enhanced expression of the *mer* gene cluster that will result in increased Hg reduction [40,41,51]. It is generally believed that microorganisms hosting *merA* have the ability to reduce Hg(II), and that Hg(II) reducing microorganisms are ubiquitous in the environment [52]. Hg reduction has been extensively studied in river/sea sediments [53–55], but linkages between Hg reduction and Hg methylation has never been studied in rice paddy soil.

Previous studies from our group focused on Hg(II) methylation and MeHg demethylation, revealing that methanogenesis play an important role in controlling MeHg concentration in rice paddy soils with methanogenesis tightly coupled to MeHg degradation [12]. In the present study we instead focus on Hg(II) and MeHg reduction and further attempt to distinguish between reductive and oxidative demethylation of MeHg along a gradient of Hg-contaminated rice paddies. The approach included the combined use of isotopically labeled tracers for different Hg species and metabolism-specific microbial inhibitors in microcosm experiments, while the produced gaseous Hg (Hg(0)) was captured and analyzed during the incubation experiment. We aimed to (i) determine Hg(II) and MeHg reduction and determine the influence of these processes on MeHg formation; (ii) predict the fate of different Hg species inputs along a gradient of Hg contamination in rice paddies; and (iii) identify and quantify the relative contribution of sulfate-reduction and methanogenesis in fueling the studied Hg transformation processes. Our results showed that the effects of Hg(II) reduction on Hg(II) methylation increased with Hg contamination level, and that sulfate-reduction and methanogenesis play important roles in both Hg(II) and MeHg reduction in rice paddy soils. The degradation of MeHg mainly take place via oxidative demethylation and didn't seem to be affected by Hg concentration. Our findings advance our understanding of Hg reduction in paddy soil, but could also guide and inform future efforts to remediate Hg contaminated paddy soil.

2. Materials and methods

2.1. Site description and sample collection

Rice paddy soils representing different levels of Hg pollution were collected from three areas in Guizhou province, southwest of China: Sikeng (an abandoned Hg mining site), Gouxi (an artisanal Hg mining site), both of which are located in the Wanshan Hg mining area, and Huaxi (a control site) situated southwest of Guiyang City, Guizhou Province (Fig. S1). The site description and the detailed sampling procedures were described in a previous work [12]. In this study, we focused on surface soil (0–2 cm below the soil-water interface) which has been identified as the most active layer of MeHg formation in rice paddy soil [12].

The surface soils and the corresponding overlaying water were sampled in the rice growing season (August 08th to 10th 2018), during when Hg methylation was active in rice paddy soil [56]. The soil samples for gene analysis were frozen in liquid nitrogen immediately after sampling. At each site, three subsamples were collected, and about 2 L of 0–2 cm top soil for each subsample thus made 6 L in total for each site. The soils were stored at 4 ℃ till further incubation experiments. The three subsamples at each site were mixed completely before the

incubation experiments were carried out, to ensure the reliability of the experiment. The pH of the corresponding overlaying water was measured on site using a portable pH meter.

2.2. Microcosm incubations setup

All the processes involved in the microcosm incubations, including soil handling and treatments, were conducted in an anaerobic chamber filled with Ar and H_2 (v:v=9:1) as illustrated in Fig. 1. The procedures for the incubation experiments and sub-sampling methods were modified from our previous studies [12,57]. Briefly, after the removal of bulky pebbles and plant roots, the paddy soil was homogenized in a 2 L beaker with the corresponding overlying water to make slurries. The water content of the slurries, determined as weight loss after drying at 60 °C until constant weight, was about 55%. Approximately 30 mL slurries were dispensed into a 100 mL serum bottle by careful pipetting, followed by the addition of specific microbial inhibitors and Hg isotope tracers according to the experimental treatments (Fig. 1). The treatments included a gradient of specific microbial inhibitors (i.e. BES and molybdate, inhibiting methanogens and SRB, respectively), combinations of two inhibitors, autoclaved controls (121 ℃ for 30 min) and reference controls (the original slurries). At the end of incubation, t samples for gene analysis were immediately frozen in liquid nitrogen and stored at − 80 °C until DNA extraction, and the samples for Hg isotopic analysis were stored at − 80 °C and freeze dried until analysis. Two Hg isotope tracers, $CH_3^{198}HgNO_3$ (98.52 ± 0.15%) and $^{202}Hg(NO_3)_2$ (98.68 ± 0.2%), were added at 100% and 10% of ambient concentrations of each site to minimize the effect of baseline Hg and MeHg concentrations [12,58], into paddy slurries to determine Hg reduction/methylation/demethylation rate constants. The isotopes were bought from ISOFLEX (San Francisco, CA, U.S.A.). $CH_3^{198}HgNO_3$ was prepared by the methylcobalamin method as described previously [12,59], and the purity (the ratio of $CH_3^{198}HgNO_3$ to total ^{198}Hg) of the synthesized $CH_3^{198}HgNO_3$ was 83.2%. All serum bottles were sealed with butyl rubber septa and aluminum crimp caps and subsequently incubated in the dark at room temperature (25 ℃) for 24 h. All reagents used in the incubation experiments were deoxygenated.

2.3. Determination of Hg reduction, methylation and demethylation rate constants in rice paddy soil

Within 5 min after tracer addition, Hg(0) from sacrificed serum bottles was purged out using N_2 and collected on a gold trap (Fig. 1) for subsequent analysis by inductively coupled plasma mass spectrometry (ICPMS, Agilent 7700x, Agilent Technologies, Inc.) [60,61]. These samples were designated as "t_1". After 24 h of incubation following Hg isotope tracer additions, the Hg(0) produced in each bottle was collected and analyzed using the same protocol as for t_1. These samples were designated "t_2". The incubation samples after purging were freeze-dried and then homogenized with a mortar and sifted through a 200-mesh sieve, followed by the analysis of MeHg isotopes by GC-ICPMS as described elsewhere [12]. There was a total of four scarified serum bottles for each treatment, one for "t_1" and three replicates for "t_2". The potential reduction rate constants of Hg(II) ($k_{re\text{-}Hg(II)}$) and MeHg ($k_{re\text{-}MeHg}$) were calculated based on the production of $^{202}Hg(0)$ (product of $^{202}Hg(NO_3)_2$ reduction) and $^{198}Hg(0)$ (product of $CH_3^{198}HgNO_3$ reduction), using Eqs. 1 and 2 [36,55], respectively. The t_1 and t_2 represents the time at the beginning and the end of incubation, respectively. The 't' represents the incubation time (day). [Hg(0)] represents the production of Hg(0), $[Hg(II)]_{(spike)}$ and $[MeHg]_{spike}$ represents the Hg isotopic tracer addition at the beginning of the incubation. Since the purity of synthesized $CH_3^{198}HgNO_3$ tracer was 83.2% as mentioned above, which means that there was 16.8% (100%−83.2%) of $^{198}Hg(NO_3)_2$ in this tracer, $^{198}Hg(0)$ would be produced from $CH_3^{198}HgNO_3$ and $^{198}Hg(NO_3)_2$. Thus, when calculating $k_{re\text{-}MeHg}$, the $^{198}Hg(0)$ produced from $^{198}Hg(NO_3)_2$ was deducted, which was described as $\left[^{198}Hg(0)\right]_{t2}^{^{198}Hg(II)}$ in Eq. (2).

$$k_{re-Hg(II)}\left(d^{-1}\right) = \frac{\left[^{202}Hg(0)\right]_{t2} - \left[^{202}Hg(0)\right]_{t1}}{\left[^{202}Hg(II)\right]_{spike} \times t} \quad (1)$$

$$k_{re-MeHg}\left(d^{-1}\right) = \frac{\left[^{198}Hg(0)\right]_{t2} - \left[^{198}Hg(0)\right]_{t2}^{^{198}Hg(II)} - \left[^{198}Hg(0)\right]_{t1}}{\left[Me^{198}Hg\right]_{spike} \times t} \quad (2)$$

The potential methylation rate constants (k_m) and potential demethylation rate constants (k_d) were calculated based on the production of $Me^{202}Hg$ and the degradation of $Me^{198}Hg$ using Eqs. 3 and 4, respectively. $[Me^{202}Hg]_{t1}$ and $[Me^{198}Hg]_{t1}$ represents the ambient concentrations of $Me^{202}Hg$ and $Me^{198}Hg$ in paddy soils, $[Me^{202}Hg]t_2$ and $[Me^{198}Hg]t_2$ represented the concentrations of $Me^{202}Hg$ and $Me^{198}Hg$ after incubation, $[^{202}Hg^{2+}]$ was the concentration of $^{202}Hg(NO_3)_2$ added into the soil.

$$\frac{k_m = \left[Me^{202}Hg\right]_{t2} - \left[Me^{202}Hg\right]_{t1}}{\left[^{202}Hg^{2+}\right] \times t} \quad (3)$$

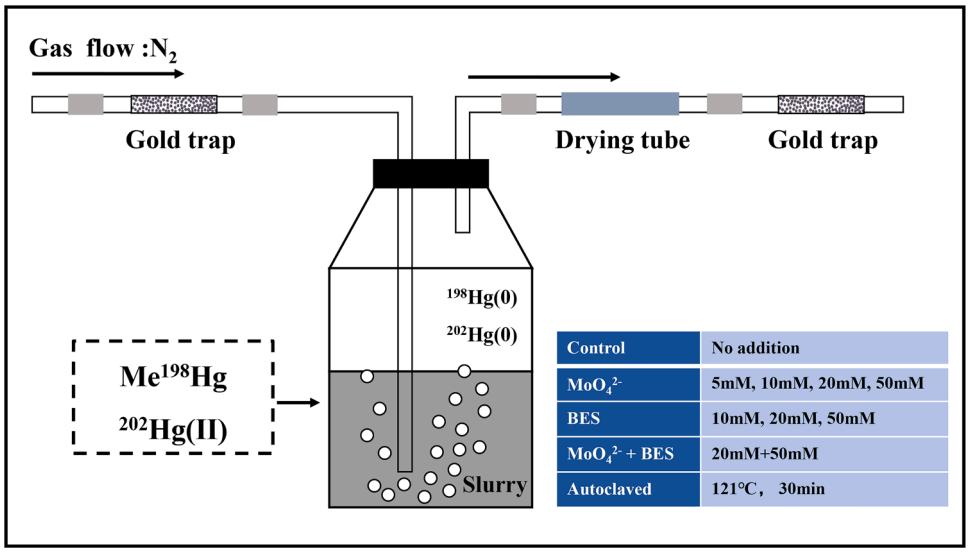

Fig. 1. Illustration of the incubation experimental set-up.

$$k_d = \frac{\ln\left(\left[Me^{198}Hg\right]_{t1}\right) - \ln\left(\left[Me^{198}Hg\right]_{t2}\right)}{t} \quad (4)$$

2.4. RNA and DNA extraction, cDNA synthesis and quantitative PCR

The field soil samples and selected incubation soil samples for DNA/RNA analyses were collected in 2 mL cryopreservation tubes, transported in liquid nitrogen immediately after collection and subsequently stored at − 80 ℃ until analysis. Total microbial RNA and DNA were extracted in triplicates from 2 g of soil using the RNeasy Power Soil Total RNA Kit (QIAGEN Inc., Germany) and DNeasy Power Soil Total RNA Kit (MoBio Laboratories, Carlsbad, CA, USA) according to the manufacturer's instructions. The concentrations and purity (A260/280) of RNA and DNA were determined using a NanoDrop 2000 spectrophotometer (Thermo Fisher Scientific, USA). The RNA samples were treated with a TURBO DNA-free™ Kit (AM1907, AMBIO, Life technologies, USA) to remove any residual DNA. The absence of DNA was verified for all samples by performing PCR using primers targeting the 16 S ribosomal RNA (rRNA) gene followed by visualization of PCR products on a 1% agarose gel stained with gel-red and detected on a UV transilluminator. The RNA was then used for synthesizing complementary DNA (cDNA) with the SuperScript™ III First-Strand Synthesis System (Super Script™ III First-Strand Synthesis Super Mix for qRT-PCR, Thermo Fisher, USA) according to the manufacturer's instructions. RNA and cDNA samples were stored at − 80 °C until further processing and analysis.

Primers used for qPCR of genes targeting microbial processes are presented in Table S1. The genomic DNA from strains purchased from DSMZ (containing the corresponding genes) were used as standards for 16 S rRNA, *dsrA* and *mcrA*. For the assays and standards of *merA* qPCR, DNA and cDNA samples were amplified using *merA* primers set (table S1), and the correct length of the PCR products was verified by GelRed-stained gel electrophoresis (2% agarose). The resulting amplicons from DNA and cDNA were purified, quantified, and prepared for serial dilution and stored at − 80 °C until use as calibration standards for qPCR and RT-qPCR quantification. All qPCR reactions were performed in 20 μl total volumes with a Bio-Rad CFX96 touch real-time PCR detection system using the commercial enzyme kit, TATAA SYBR® GrandMaster® Mix (TATAA Biocenter AB, Sweden) in accordance with the manufacturer's recommendations. Positive (standard samples) and no-template controls were included in each qPCR run. The copy numbers of target genes per sample were calculated, and the quality of the standard curve and melting curves were tested as described elsewhere [62,63].

PCR reactions for both samples and standards were carried out in triplicate. The qPCR amplification reactions and thermal programs for all the studied genes are presented in Table S1 and Table S2, respectively. The amplification efficiency of standards and linear dynamic range for the different assays are shown in Table S3.

2.5. Chemical analysis

THg and MeHg concentrations were determined using the previously described method [64]. Hg(0) collected on gold traps was analyzed by ICPMS as described above. We obtained the standard curve ($r^2 > 0.999$) of Hg (0) by $SnCl_2$ and Hg standard solution (1 ng·mL^{-1}). Sulfur K-edge X-ray absorption near edge spectroscopy (XANES) of the paddy soil samples was performed at the Beijing Synchrotron Radiation Facility (BSRF) using the method as described elsewhere [65]. Sulfide (S^{2-}) and Fe^{2+} concentrations in pore water were measured using the methylene blue method [66] and Colorimetric o-Phenanthroline Method [67] method, respectively. Briefly, the pore water was obtained by centrifuging the paddy soils at 3000 rpm for 30 min, followed by filtering through 0.45 μm. For S^{2-} analysis, the pore water was treated with N, N-dimethyl-p-phenylenediamine solution and $FeCl_3$ solution, which was then purged with N_2 for about 30 s and sealed tightly with the lid, S^{2-} concentration was measured by determining the absorbance at 667 nm on a UV–vis spectrometer (UV-5100, METASH, China). Pore water treated with 25% HCl, 0.5% o-phenanthroline, CH_3COONa and CH_3COOH-CH_3COONH_4 buffer were prepared to measure absorbance at 667 nm to determine Fe^{2+} concentration. The production of methane (CH_4) and carbon dioxide (CO_2) during incubation were measured from the head space by taking 10 mL gas using syringe and subsequent analysis by gas chromatography (GC 6890, Agilent, America). Standard gases of CH_4 and CO_2 were obtained from China reference material center.

2.6. QA/QC

Method blanks, triplicates and certified reference material were used for quality control and assurance measurements. Quantitative determination of Hg(0) isotopes was based on standard calibration curves, $r^2 \geq 0.999$. Quantification for Fe^{2+} and S^{2-} in pore water was conducted using daily calibration curves with the coefficient of variation (r^2) ≥ 0.99. The method detection limit (3σ) for Hg(0) isotope analysis was 0.047 pg. Methane and carbon dioxide standard gases are sourced from the China Reference Materials Center. Quality analysis was performed with SPSS 22.0 software. A one-way ANOVA (Dunnett's test, $p < 0.05$) was used to test for significant differences between controls and other treatments. Significant differences of gene copy numbers between different sampling sites were determined using a Tukey post-hoc test ($p < 0.05$). Pearson's correlation coefficients ($p < 0.05$ and $p < 0.01$) were used to describe the linear dependence (correlation) between variables. Redundancy analysis (RDA) conducted with the Canoco 5.0 software was used to extract and summarize the variation in the set of variables by another set of explanatory variables.

3. Results

3.1. Physical and chemical properties of the rice paddy soils

Along the Hg contamination gradient, the pH of overlying water was significantly higher at Sikeng (9.87 ± 0.26) compared to Huaxi (8.23 ± 0.58) and Gouxi (7.41 ± 0.02) (Table 1). Fe^{2+} concentrations in pore water were highest at Huaxi (95.52 ± 12.70 μM), followed by Gouxi (33.24 ± 12.97 μM) and Sikeng (11.93 ± 3.90 μM) (Table 1). S^{2-} concentrations in pore water, indicative of dissimilatory sulfate reduction, showed no significant difference across the three sites (Table 1). CH_4 concentrations in the soil incubations from Huaxi (13,268 ± 220 mg·L^{-1}) were significantly higher than corresponding estimates from Sikeng (9458 ± 396 mg·L^{-1}) and Gouxi (5339 ± 368 mg·L^{-1}). In contrast, CO_2 concentrations were highest at Sikeng (28,058 ± 174 mg·L^{-1}), followed by Gouxi (16,577 ± 256 mg·L^{-1}) and Huaxi (15,836 ± 235 mg·L^{-1}). The chemical speciation of sulfur in the paddy soil was dominated by oxidized S, with sulfate and methanesulfonate representing > 50%, while organic reduced S (L-Cysteine and DL-methionine sulfoxide) accounted for 23~26%, and RSH and Zero-valent S (Sulfur) 20~22% and 19~21% (Tables 2 and 3), respectively.

3.2. Hg(II) reduction rate constants ($k_{re\text{-}Hg(II)}$)

Hg(II) reduction rates ($k_{re\text{-}Hg(II)}$) in the control treatment varied greatly (up to three orders of magnitudes) along the Hg contamination gradient (Fig. 2). The highest $k_{re\text{-}Hg(II)}$ were observed at the control site Huaxi ((14.04 ± 0.77) × 10^{-5} d^{-1}), while the lowest were observed at the artisanal mining site Gouxi ((0.0071 ± 0.001)× 10^{-5} d^{-1}). Sikeng, an abandoned Hg mining site with the highest THg concentration, had intermediate Hg(II) reduction rates ((0.073 ± 0.03) × 10^{-5} d^{-1}). Hg(II) reduction across all the sites was almost completely suppressed by autoclaving (Fig. 2a, b and c).

The effects of molybdate and BES on Hg(II) reduction varied among sites (Fig. 2a, b and c). At Huaxi, Hg(II) reduction was significantly inhibited by molybdate (Mo) amendments, with Hg(II) reduction rates

Table 1
The physical and chemical parameters of rice paddy soil. The spiked with a, b and c represent significant differences among three studied sites (Turkey test, $p < 0.05$).

Sites	THg* ($mg \cdot kg^{-1}$)	MeHg* ($\mu g \cdot kg^{-1}$)	Fe^{2+} (μM)	S^{2-} (μM)	CH_4 ($mg \cdot L^{-1}$)	CO_2 ($mg \cdot L^{-1}$)	pH
Huaxi	0.46 ± 0.01^a	0.96 ± 0.24^b	95.52 ± 12.70^a	0.24 ± 0.11^a	$13{,}268 \pm 220^a$	$15{,}836 \pm 235^c$	8.23 ± 0.58^b
Gouxi	37.16 ± 31.46^a	2.07 ± 1.23^a	33.24 ± 12.97^b	0.31 ± 0.21^a	5339 ± 368^c	$16{,}577 \pm 256^b$	7.41 ± 0.02^b
Sikeng	65.75 ± 46.19^a	0.98 ± 0.25^b	11.93 ± 3.90^c	0.18 ± 0.00^a	9458 ± 396^b	$28{,}058 \pm 174^a$	9.87 ± 0.26^a

*Reference to a companion study [12].

Table 2
The percentage of different S speciation in total soil S determined by Sulfur K-edge XANES. The L-Cysteine, DL-methionine sulfoxide, Na Methanesulonate, Na_2SO_4, Sulfur and RSH were sulfur speciation, represent the percentage in total soil S (%), determined by Sulfur K-edge XANES. The spiked with a, b and c represent significant differences among three studied sites (Turkey test, $p < 0.05$).

Sites	L-Cysteine (%)	DL-methionine sulfoxide (%)	Na Methane sulonate (%)	Na_2SO_4 (%)	Sulfur (%)	RSH (%)
Huaxi	$21 \pm 4\%^a$	$5 \pm 2\%^a$	$31 \pm 1\%^a$	$24 \pm 3\%^a$	$19 \pm 4\%^a$	$21 \pm 4\%^a$
Gouxi	$20 \pm 6\%^a$	$3 \pm 2\%^a$	$31 \pm 2\%^a$	$25 \pm 3\%^a$	$21 \pm 6\%^a$	$20 \pm 6\%^a$
Sikeng	$22 \pm 0\%^a$	$3 \pm 3\%^a$	$33 \pm 2\%^a$	$24 \pm 3\%^a$	$19 \pm 3\%^a$	$22 \pm 0\%^a$

decreasing with increasing Mo concentrations (Fig. 2a). BES amendments had no significant effects on Hg(II) reduction, with the exception that an addition of 20 mM BES significantly enhanced Hg(II) reduction. The combination of Mo+BES significantly inhibited Hg(II) reduction at the Huaxi site (Fig. 2a).

At Gouxi, molybdate amendments instead greatly enhanced Hg(II) reduction, but with Hg(II) reduction rates gradually decreasing with the increasing concentration of Mo (Fig. 2b). Hg(II) reduction rates were also significantly elevated by BES amendments, while the combination of Mo+BES had no apparent effect on Hg(II) reduction (Fig. 2b).

At the Sikeng site, Hg(II) reduction was greatly suppressed by all molybdate amendments, either alone or in combination with BES. BES amendments alone had no effects on Hg(II) reduction at Sikeng (Fig. 2c).

3.3. MeHg reduction rate constants ($k_{re\text{-}MeHg}$)

We also determined the degradation of MeHg to Hg(0) as a MeHg reduction rate constant ($k_{re\text{-}MeHg}$). Our results showed that $k_{re\text{-}MeHg}$ in the controls at Huaxi, Gouxi and Sikeng were $(3.00 \pm 0.27) \times 10^{-5}$ d^{-1}, $(4.39 \pm 0.02) \times 10^{-5}$ d^{-1} and $(4.87 \pm 0.45) \times 10^{-5}$ d^{-1}, respectively. Hence there were no significant difference between sites (Fig. 2d, e, f). Autoclaving significantly decreased $k_{re\text{-}MeHg}$ by 61%, 75% and 54% compared to the controls in Huaxi, Gouxi and Sikeng, respectively (Fig. 2d, e, f).

Similar to Hg(II) reduction, the effects of different inhibitors on MeHg reduction varied between sites (Fig. 2d, e, f). At Huaxi and Gouxi, the amendments of 5, 10 and 50 mM molybdate increased $k_{re\text{-}MeHg}$ (Fig. 2d, e). Surprisingly, the 20 mM molybdate treatment significantly inhibited $k_{re\text{-}MeHg}$ ($p < 0.05$, Fig. 2d, e). At Sikeng, $k_{re\text{-}MeHg}$ was significantly inhibited by molybdate at all the concentrations applied, and the degree of inhibition increased with inhibitor concentrations ($p < 0.01$, Fig. 2 f). BES also inhibited $k_{re\text{-}MeHg}$, and the extent of inhibition increased with BES concentration (Fig. 2d, e, f), except for BES-10 mM at Gouxi.

3.4. Influence of Hg(II) and MeHg reduction on MeHg formation in rice paddy soils

Since Hg(II) reduction and methylation compete for the substrate, the Hg(0)/MeHg ratio of the products will, to some extent, reflect the influence of Hg(II) reduction on methylation. The ratio of $^{202}Hg(0)/Me^{202}Hg$ produced from the enriched $^{202}Hg(NO_3)_2$ were 0.4%, 0.03% and 6% in Huaxi, Gouxi and Sikeng, respectively. The values of $^{202}Hg(0)/Me^{202}Hg$ at Huaxi and Gouxi were relatively low compared to Sikeng.

As described above, MeHg can be demethylated to Hg(0) or Hg(II) by RD and OD, respectively. In all three sites, the $^{198}Hg(0)$ produced from the enriched $CH_3^{198}HgNO_3$ was much lower than $^{198}Hg(II)$ produced (Fig. S2), suggesting that OD is the dominant sink for MeHg. The ratios of $^{198}Hg(0)$ to $^{198}Hg(II)$ were 0.006%, 0.008% and 0.007% at Huaxi, Gouxi and Sikeng, respectively (Fig. S2).

3.5. Expression of Hg transforming genes and some related functional genes (merA, SRB-Firm hgcA, Archaea-hgcA, 16 S rRNA, dsrA, mcrA)

We characterized the expression of *merA* (Hg reductases), SRB-Firm *hgcA* (Hg methylating firmicutes), Archaea *hgcA* (Hg methylating archaea), *dsrA* (sulfate reductase), *mcrA* (methanogensis) and 16 S rRNA as markers for general bacterial activity of the corresponding pathways in some selected incubation and field sample of rice paddy soils (Fig. 3). In line with other studies [43], *merA* copy numbers from the field DNA samples significantly increased with Hg-contamination level, with $(2.10 \pm 0.64) \times 10^6$, $(4.95 \pm 0.61) \times 10^6$ and $(12.74 \pm 2.11) \times 10^6$ copies per gram fresh soil from Huaxi, Gouxi and Sikeng, respectively

Table 3
Comparison of k_m and k_d values in different types of wetlands among different countries.

Wetland types	MeHg/THg (%)	k_m (10^{-3} day^{-1})	k_d (day^{-1})	Hg (II) volatilize/reduction rate	References
Rice paddy soils (Huaxi)	0.27 ± 0.05 (0–2 cm)	24.45 ± 3.73 (0–2 cm)	0.77 ± 0.12(0–2 cm)	$(14.44 \pm 0.77) \times 10^{-5}$ d^{-1} (3.18%) (0–2 cm)	[12]
Rice paddy soils (Gouxi)	0.08 ± 0.02(0–2 cm)	0.15 ± 0.06(0–2 cm)	0.68 ± 0.01(0–2 cm)	$(0.0071 \pm 0.001) \times 10^{-5}$ d^{-1} (0.02%)(0–2 cm)	[12]
Rice paddy soils (Sikeng)	0.002 ± 0.001 (0–2 cm)	0.032 ± 0.016 (0–2 cm)	0.85 ± 0.03(0–2 cm)	$(0.073 \pm 0.03) \times 10^{-5}$ d^{-1} (0.0001%)(0–2 cm)	[12]
Peat	0.03–0.37	1–100	0.0015–0.004	——	[57]
Estuarine sediments	——	0.1035 $g^{-1} \cdot h^{-1}$	0.379 $g^{-1} \cdot h^{-1}$	0.0033%	[53]
Sea sediments	~0.1 (0–2 cm)	~2.5 (0–2 cm)	~0.25 (0–2 cm)	$\sim 0.5 \times 10^{-5}$ d^{-1} (0–2 cm)	[55]
poor nutrient wetlands	4.5 ± 0.90–5.1 ± 0.83	11 ± 2.3–38 ± 10	0.027 ± 0.0076 – 0.11 ± 0.065	——	[68]
nutrient richer wetlands	2.3 ± 0.51–5.2 ± 1.4	22 ± 5.4–57 ± 11	0.047 ± 0.026 – 0.091 ± 0.052	——	
High Arctic wetland	0.6–18.5 (0–2 cm)	71 ± 60 (0–2 cm)	0.023 ± 0.028% (0–2 cm)	——	[69]
Vernon Lake	——	16	0.528	——	[36]
Florida Everglades Peat	0.1–1.7 *	20 (0–120)	0.007 ± 0.002–0.060 ± 0.007	——	[60,70]

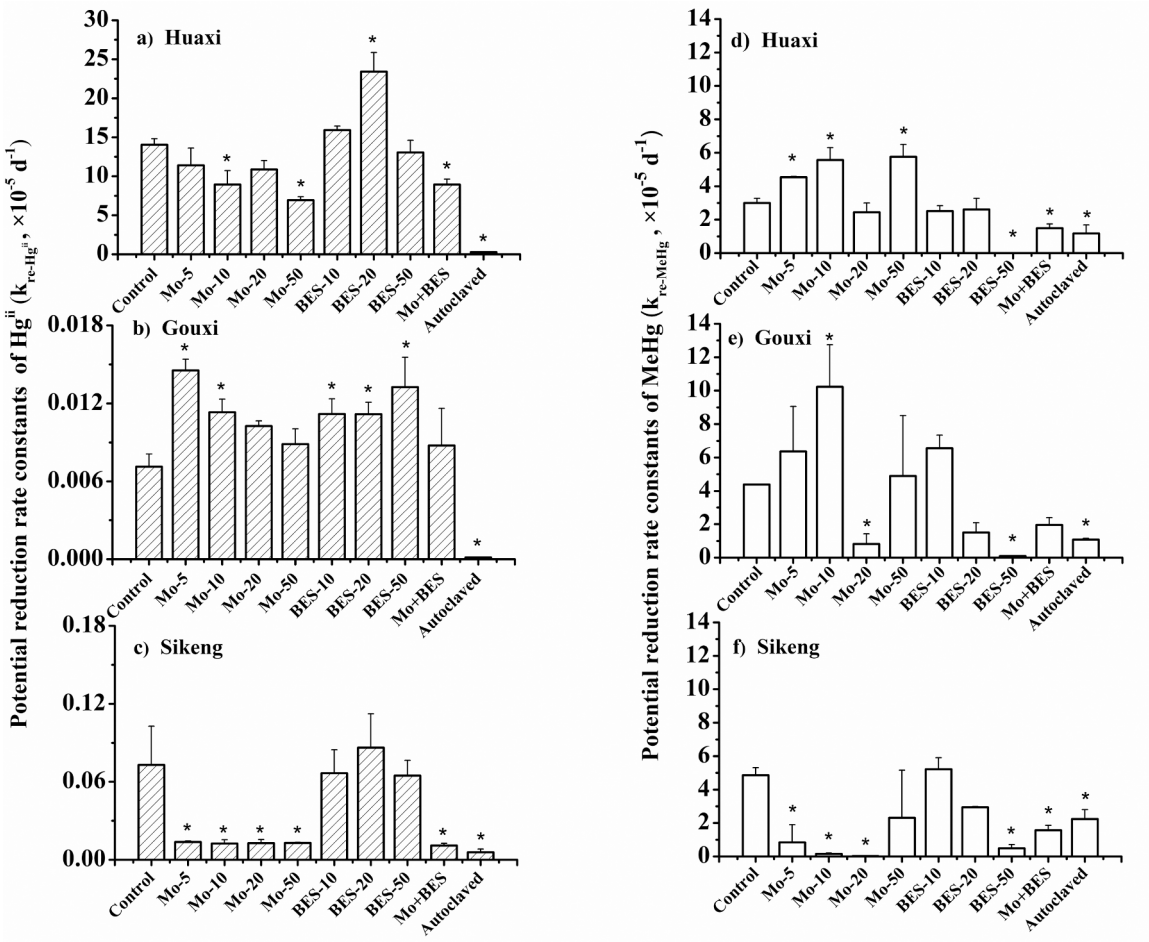

Fig. 2. Potential reduction rate constants of Hg(II) ($k_{re\text{-}Hg(II)}$ ± STD, n = 3) and MeHg ($k_{re\text{-}MeHg}$ ± STD) in rice paddy soils across a Hg contamination gradient under different treatments. Huaxi (a and d, the control site); Gouxi (b and e, the artisanal Hg mining site); Sikeng (c and f, the abandoned Hg mining site). The numbers of 5, 10, 20 and 50 following Mo and BES indicated the concentrations of each inhibitor (mM) we added in the incubations. Mo+BES: combination of 20 mM molybdate and 50 mM BES. Autoclaved: 121 ℃, 30 min. An asterisk denotes significant difference from control treatment (n = 3, Dunnett's test, $p < 0.05$).

(Fig. 3a, $p < 0.05$). The *merA* transcripts (RNA samples) were (0.53 ± 0.32) × 10^4, (0.69 ± 0.26) × 10^4 and (1.90 ± 1.99) × 10^4 per gram fresh soil at Huaxi, Gouxi and Sikeng, respectively, thus featuring an increase with higher Hg levels, even if the difference was not statistically significant at the 5% confidence level (Fig. 3a). As expected, *merA* copies in DNA were two orders of magnitude higher than in RNA, suggesting that the expression of *merA* (the ratio of *merA* in RNA to in DNA) was generally low in rice paddies (Fig. 3a, $p < 0.05$). Furthermore, *merA* transcripts in all the selected incubation samples were also very low, i.e. below or close to the detection limit (data not shown). Hence *merA* did not seem to be actively expressed under anaerobic conditions, which is in agreement with a widely recognized role of *merA*-dependent reduction taking place in aerobic settings.

The expression *of hgcA* genes from Archaea, SRB and firmicutes were detected in paddy soil incubations (Fig. 3b-c). SRB-firmicutes *hgcA* transcripts were highest at Huaxi (4.62 ± 1.96 ×10^5 copy/g), followed by Gouxi (3.17 ± 2.35 ×10^5 copy/g) and Sikeng (2.41 ± 0.46 ×10^5 copy/g) (Fig. 3b). At Sikeng, BES, which inhibit methanogenesis, greatly increased the expression of SRB-firmicutes *hgcA,* revealing the competitive relationship between these two microbial metabolic guilds. Archaeal *hgcA* transcript were highest at Huaxi (9.40 ± 2.64 ×10^5 copy/g), followed by Sikeng (4.87 ± 1.88 ×10^5 copy/g) and Gouxi (0.9 ± 0.19 ×10^5 copy/g). Hg methylation by methanogens was lowest at Gouxi, which is consistent with *mcrA* expression indicative of methanogenic activity.

The highest 16 S rRNA gene expression was found at Sikeng ((6.53 ± 2.27) × 10^9 copy g^{-1} soil), followed by Gouxi ((4.04 ± 0.85) × 10^9 copy g^{-1} soil) and Huaxi ((0.3 ± 0.15) × 10^9 copy g^{-1} soil), with a general a pattern of increasing 16 S rRNA expression with increasing Hg-contamination. This suggests that general microbial activity and/or biomass may increase with Hg-contamination level. At Huaxi and Sikeng, the addition of Mo and/or BES greatly increased 16 S rRNA levels, especially for the Mo+BES treatments (Fig. 3d, $p < 0.01$). At Gouxi, this proxy of microbial activity was greatly inhibited by BES-50, while Mo-20 and Mo+BES had no effect. For Sikeng we observed the opposite response, with microbial 16 S rRNA levels being depressed by Mo-20 and enhanced by BES-50 and Mo+BES (Fig. 3d). A similar trend was observed both at low (Huaxi) and high (Sikeng) Hg concentrations suggesting that enhanced ribosome synthesis is likely a direct response to inhibition of SRBs and methanogens. We were unfortunately not able to identify the microbes who increasing their 16 S rRNA production in response to this metabolic guild inhibition.

Huaxi had the highest *dsrA* transcripts (6.78 ± 1.15 ×10^3 copy g^{-1}), followed by Gouxi (2.66 ± 0.57 ×10^3 copy g^{-1}) and Sikeng (2.18 ± 0.17 ×10^3 copy g^{-1}) (Fig. 3e). Sulfate reduction activity decreased in response to the Mo+BES treatment, and similar patterns were observed for Hg(II) reduction rate constants as mentioned above. It is worth noting that *dsrA* transcripts increased with BES amendments at all sites, supporting the competition between SRBs and methanogens. Similarly, Huaxi had the highest *mcrA* transcript (21.65 ± 5.47 ×10^3 copy g^{-1}), followed by Sikeng (5.30 ± 1.48 ×10^3 copy/g) and Gouxi (1.27 ± 0.44 ×10^3 copy/g) (Fig. 3 f). Both molybdate and BES treatments

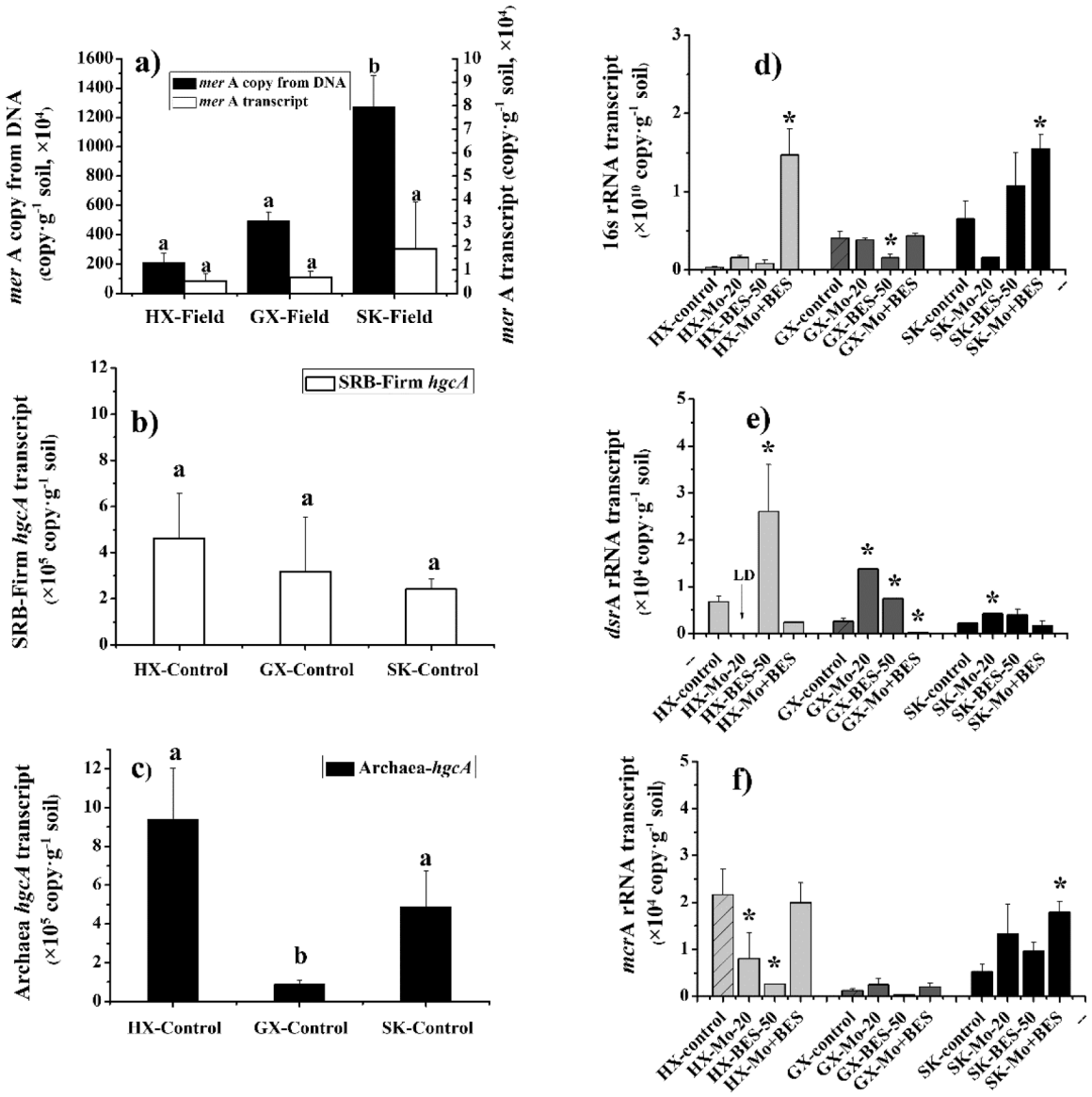

Fig. 3. (a) The abundance and transcript of *merA* for the in situ samples, (b) transcripts of SRB-Firm *hgcA*, (c) Archaea *hgcA*, (d)16 s rRNA (the total microbial activity), (e) *dsrA* (the SRBs' activity) and (f) *mcrA* (the methanogens' activity) in some selected incubations of rice paddy soils measured by RT-PCR. HX, GX, and SK from the labels of x-axis indicate Huaxi, Gouxi and Sikeng site, respectively. The samples in Fig. 3a are field soil samples, while Fig. 3b, c, d, e and f show the soil samples after incubation. Markings of "a", "b", and "c" above the bars indicate a significant difference (Tukey post-hoc test, $p < 0.05$, n = 3). An asterisk denotes significant difference from each control treatment, $p < 0.05$. The labels on the x-axis are the same as for Fig. 2.

significantly inhibited *mcrA* transcripts at Huaxi (Fig. 3 f, $p < 0.05$), indicating that there were some interactions between SRB and methanogens at this site.

Global analysis of parameters measured in rice paddy soil was further conducted with redundancy analysis (RDA) analysis (Fig. 4). The first dimension in the ordination account for 62.47% of the variation while the second dimension account for 19.33%. The k_m (1^{**}), $k_{re\text{-}MeHg}$ (0.90^{**}), Fe^{2+} concentration (0.95^{**}), CH_4 production (0.85^{**}) and expression of *mcrA* (0.94^{**}), *dsrA* (0.95^{**}), *archaea-hgcA* (0.80^{**}) were positively correlated with $k_{re\text{-}Hg(II)}$ (Table S5). Our analysis suggest that Hg reducing and methylating microorganisms were active in the background area (Huaxi), while the *merA* gene for Hg demethylation was more highly expressed at the most Hg contaminated site (Sikeng). The pearson correlation coefficient furthermore revealed a strong negative correlation (−0.73 *, Table S5) between MeHg and k_d for the studied sites suggesting that demethylation may play a quantitatively significant role.

3.6. Fate of newly imported Hg(II) and MeHg

We calculated the portions of each transformation to predict the fate of newly external input and/or formed Hg(II) and MeHg (Fig. 5) in rice paddies, including MeHg demethylation/reduction and Hg(II) methylation/reduction. During the 24 h incubation period, 48%, 56% and 73% of the spiked MeHg representing such external inputs, were demethylated to Hg(II), while only 0.003%, 0.004% and 0.005% of the MeHg were reduced to Hg(0) at Huaxi, Gouxi and Sikeng, respectively (Fig. 5a, b and c). The demethylation (produced Hg(II)) increased along the Hg contamination gradient, while reduction (produced Hg(0)) was similar among sites. Besides the reduction to Hg(0) and demethylation to Hg(II), a pool of MeHg seem to be retained in the ecosystem, possibly because of combine with soil organosulfur-containing compounds unavailable for biological use [71], or assimilation by plants roots. Unlike MeHg, more than 96% of the spiked Hg(II) was retained in the paddy soils (Fig. 5d, e and f). This indicates that newly deposited Hg rapidly combines with

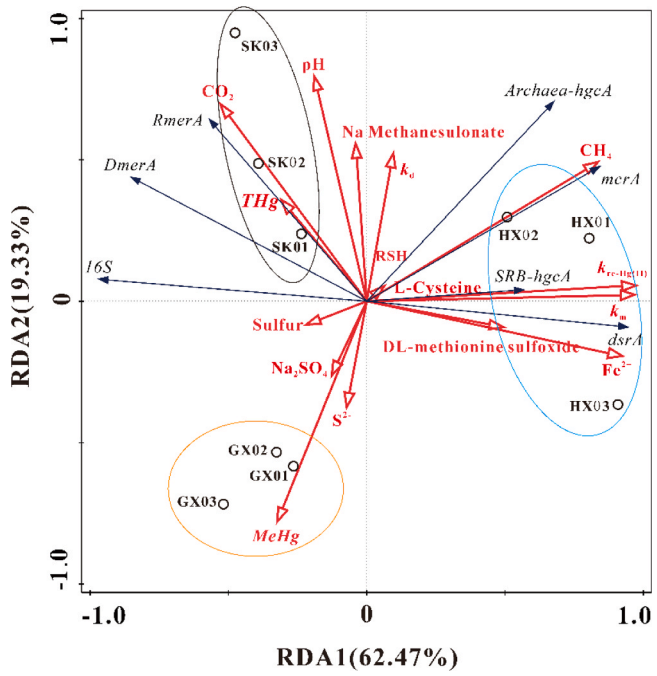

Fig. 4. RDA analysis (b) of physico-chemical parameters for studied paddy soils: HX (Huaxi), GX (Gouxi) and SK (Sikeng).

various soil constituents to form biologically recalcitrant compounds, e.g HgS and HgO, that are less accessible for microbial methylation or reduction [72]. Although most spiked Hg(II) was not available, there were still 3.18%, 0.02%, 0.003% of the Hg(II) methylated to MeHg, and 0.013%, 0.000007%, and 0.00007% of Hg(II) reduced to Hg(0) at Huaxi, Gouxi and Sikeng, respectively (Fig. 5d, e and f).

4. Discussion

4.1. Microbial guilds involved in Hg(II) reduction in rice paddy soils

After adding ^{202}Hg(II) as a Hg methylation tracer for the 24 h incubations, ^{202}Hg(0) was rather surprisingly observed in the headspace of the serum bottles. The production of Hg(0) also varied between treatments. The production of Hg(0) during Hg transformations has often been overlooked in Hg research. The present study quantifies the Hg(0) production and evaluates its impact on the occurrence of different forms of Hg in nature.

Our observations suggest that sulfate-reduction was likely the main microbial process controlling Hg(II) reduction at Huaxi and importantly also at the more contaminated Sikeng site. The role of sulfate reduction as a driver of Hg(II) reduction at the Gouxi site remains unclear, with reduction rates also being the lowest for the three sites studied. It was surprising to observe such low reduction rates at Gouxi, a site where we previously measured robust Hg methylation and anaerobic microbial activity [12,34,73]. Gouxi is unique in that it exhibits high atmospheric Hg(0) levels resulting from the artisanal mining activities. Unfortunately, the role of elevated $Hg(0)_{atm}$ levels on Hg redox processes in soil remains poorly understood.

BES addition used for inhibition of methanogenesis, didn't affect Hg (II) reduction at any of the sites, suggesting that methanogens have no or only a weaker or more long-term indirect effect on Hg(II) reduction by competing with Hg reducing SRB and iron reducers for organic substrates [28,74]. Alternatively, methanogens may also be capable of Hg (0) oxidation under anaerobic conditions, as previously observed for some SRBs and iron reducing bacteria [28], limiting our ability to observe any net effect on Hg(0).

There was an order of magnitude difference in Hg(II) reduction rates between the different sites along the Hg contamination gradient with Huaxi > Sikeng > Gouxi. Intriguingly, the lowest $k_{re\text{-}Hg(II)}$ was observed at the Gouxi site (intermediate Hg concentrations). Fe^{2+} concentrations can reveal the activity of iron-reducers known to be important Hg reducing microorganisms [75,76]. The highest Fe^{2+} level at the Huaxi site indicated that iron reducers may be particularly active at the Huaxi site (non-Hg contaminated site). Accordingly, we suggest that the higher Hg reduction rates at Huaxi may be related to an enhanced activity of iron reducing bacteria.

We observed that the Hg(II) reduction had a low effect on Hg(II) methylation at low Hg-contaminated sites. The more available Hg(II) for methylation, the more *hgc*A expression by microorganisms (Fig. 4b and c). While the proportion of Hg(II) reduction to methylation can reach up to 13.6% at high Hg-contaminated sites. The less available Hg(II) leads to a decrease in methylation substrates, resulting in a decrease in the expression of *hgc*A (Fig. 4b and c). The varies of Eh can affect the

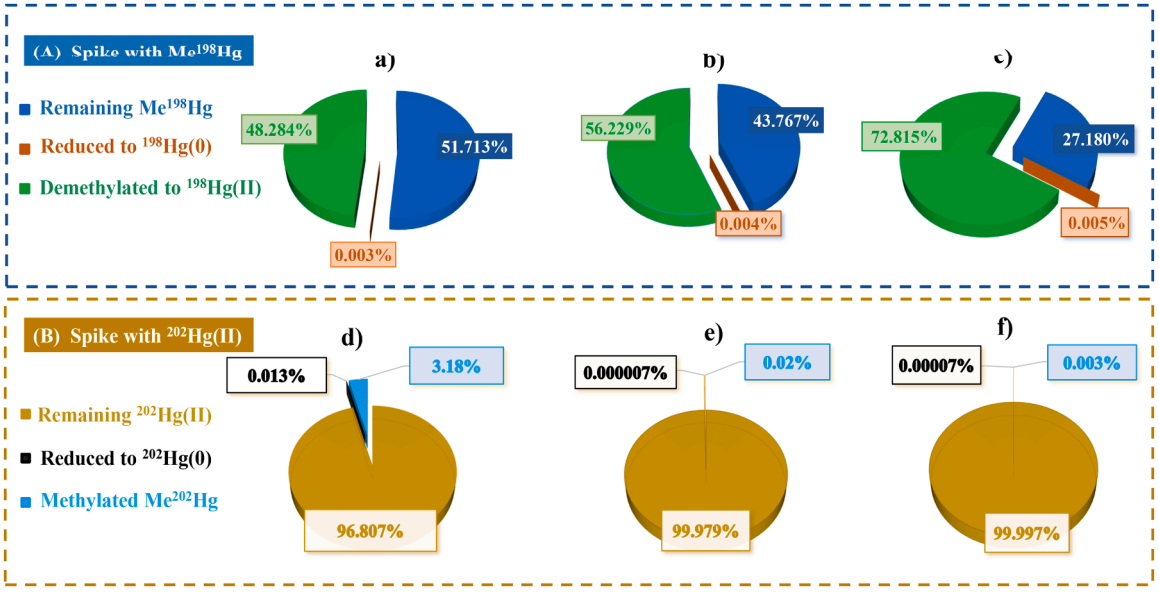

Fig. 5. The fate of the isotopic tracers of $Me^{198}Hg$ (A: a, b, c) and ^{202}Hg(II) (B: d, e, f) amended in a gradient of Hg contaminated rice paddy soils after spiking in the microcosm incubations for 24 h. Huaxi (a and d, the control site); Gouxi (b and e, the artisanal Hg mining site); Sikeng (c and f, the abandoned Hg mining site).

abundance of methylation microorganisms [15,16]. Redox variations seem to affect the biogeochemical behavior of dissolved inorganic Hg species and MeHg indirectly through related changes in DOC, sulfur cycle [77]. Therefore, redox should be taken into account when exploring the factors affecting microbial methylation in rice paddy soil in the future.

4.2. MeHg degradation: oxidative VS reductive demethylation in rice paddy soils

Our results showed that OD is absolutely dominant MeHg demethylation in both highly contaminated and less Hg contaminated paddy soils, with methanogens and SRBs being involved in OD. Oxidative MeHg demethylation has been described for methanogens and SRB that do not typically have genetic *mer*-operon determinants and for which the final product is Hg(II) rather than Hg(0) [39,70,78]. The methanogens may degrade MeHg via a pathway analogous to monomethylamine ($CH_3NH_3^+$) degradation, which decomposes MeHg (CH_3Hg^+) to CH_4 and Hg(II). SRBs may decompose MeHg into CO_2 and Hg(II) through a process similar to acetate degradation.

The presence of *mer* determinants in anaerobes is rare and the functional potential of the few "*MerA*-like" proteins found in anaerobe genomes remains questionable without proper experimental validation [70,78,79] Hg(II), the product of OD, is also subject to re-methylation within the sediment community. Thus, a cryptic methylation-demethylation cycle may exist in environments lacking the *mer*-mediated process [43]. Several environmental studies [39,78,80] suggest that *mer*-mediated RD dominate at high Hg concentrations in more aerobic settings, whereas OD dominate at lower Hg concentrations in anaerobic conditions [43]. Thus, conditional inductibility of the *mer* operon may critically affect MeHg production in Hg-contaminated environments.

In addition, there may exist some abiotic demethylation processes in paddy soils. MeHg can react with H_2S or sulfide minerals to form HgS(s) and dimethylmercury ($(CH_3)_2Hg$) [81,82]. MeHg can also react with selenoamino acids leading to the formation of HgSe(s) [83,84]. Otherwise, the relative abundance of demethylation bacteria (Clostridium spp.) significantly decreased at a high Eh value in paddy soil [15]. The abiotic system of demethylation processes in paddy field is worthy of further exploration.

4.3. The Hg biogeochemical cycle in rice paddy soils

Summarizing the observations from the present study and the previous work [12,85,86], we propose a conceptual Hg cycle in rice paddy soil, including the transformations of Hg methylation, demethylation, reduction and absorption, in which the ratios of each pathway and the relative contributions of different microbial metabolisms to each pathway are estimated as shown in the Fig. 6. In the estimation, the reference site (Huaxi) was applied and the total amount of Hg(II) input into the paddy soil was assumed as 100%. MeHg demethylation in soil accounts for ~48% (1.54/3.18) of Hg(II) methylation, suggesting long term accumulation of MeHg in the paddy soil. In the process of Hg methylation and demethylation, there is also Hg reduction, whereby both Hg(II) (~0.013%) and MeHg (~0.0001%) can be reduced to Hg(0). After volatilized Hg(0) enters the atmosphere, it can be transported over a long distance with the atmospheric circulation [87], or subsided into the paddy soil. Due to the low volatilization rate, paddy soil is a weak source of atmospheric Hg emissions, resulting in the formation of mercury sinks in paddy soil. A previous study of field plot experiments using stable Hg isotope tracers suggest that the absorption of Hg(II) and MeHg input by rice plants were ~0.9% and ~0.5%, respectively [86]. For non-Hg contaminated sites, there is a high Hg methylation rate in paddy soils. Once there is new input of Hg, it will be methylated immediately, increasing ecological risks.

The relative contributions of sulfate-reduction and methanogenesis, which were largely recognized as important processes for controlling MeHg level in rice paddy soils, on Hg transformations were estimated by combining the present and a parallel study [12]. At Huaxi (the background site), sulfate-reduction contributes ~51%, 63% and 41% to microbial Hg(II) reduction, Hg(II) methylation and MeHg demethylation, respectively. Methanogenesis contributes ~100% to MeHg reduction to Hg(0) and ~66% to MeHg degradation to Hg(II), showing the vital role of methanogenesis on MeHg degradation.

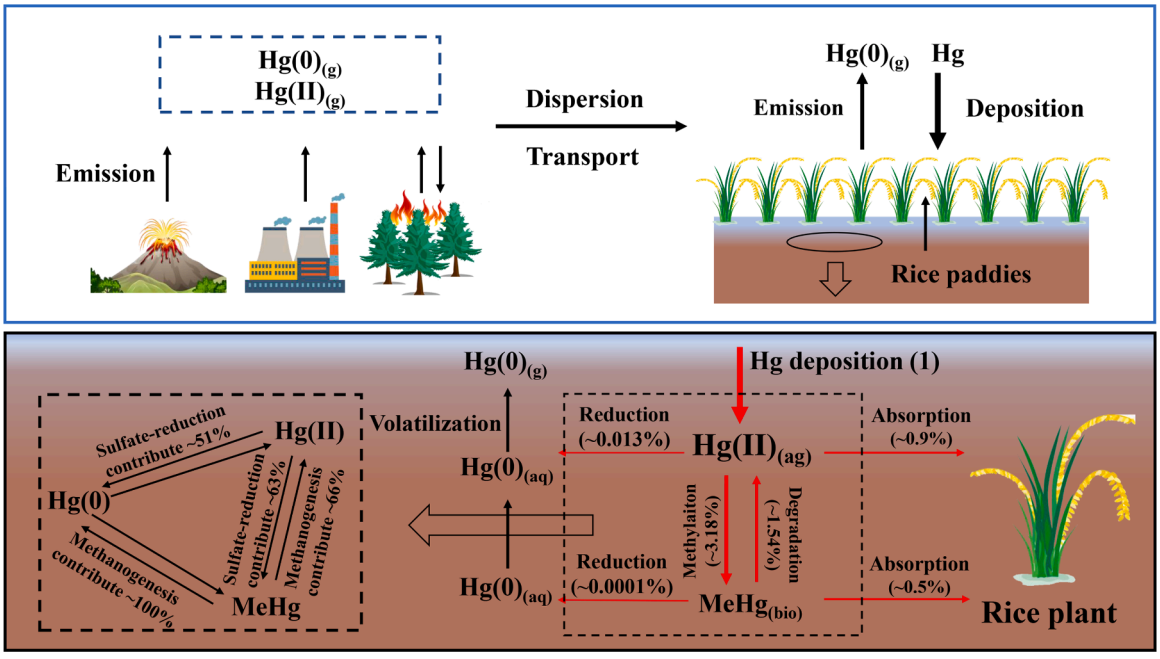

Fig. 6. Hg cycling in rice paddy soils. Transformation ratios are relative to the control site (Huaxi) in this study, which represents most of the worldwide rice growing area. The absorption ratios of Hg(II) (0.9%) and MeHg (0.5%) by mature rice plants (110 days after planting) were calculated from a previous study in our group [86], while other transformation and transportation ratios were calculated based on the present study.

Previous studies have typically targeted only one or at most two transformation processes, e.g. methylation or demethylation or reduction, and this study is to the best of our knowledge the first to simultaneously summarize the complex cycling pathways and also quantify each pathway, providing a comprehensive and broader understanding of Hg cycling in rice paddy soils.

5. Conclusion

In our incubation experiments, Hg(II) and MeHg reduction in rice paddy soils were greatly decreased by the specific microbial metabolism inhibitors for SRB and methanogens. This indicates that sulfate-reduction and methanogenesis play an important role in the Hg(II) and MeHg reduction in rice paddy soils. Microbial activities controlled the anaerobic Hg reduction processes in rice paddy soils, which was explained by the fact that $k_{re\text{-}MeHg}$ and $k_{re\text{-}Hg(II)}$ were significantly inhibited by autoclaved treatment. Furthermore, oxidative demethylation was the dominant MeHg microbial degradation pathway in paddy soils, compare to reductive demethylation. Hg(II) reduction restricted the amount of Hg(II) available for methylation at the high Hg-contaminated site. This may be one crucial factor making paddy soils a hotspot for Hg(II) methylation.

Soils were incubated anaerobically in sealed bottles for only 24 h in our experiments. These conditions are much more stable than the natural environment, e.g. Hg availability varies with redox due to weather impacts, flooding-drying cycles and other soil management practices invoked by rice cultivation. Notably, the control site featured the highest Hg methylation and reduction rates for inorganic Hg, suggesting that new inorganic Hg inputs to such paddy soils will cause higher levels of volatile Hg(0) and potential risks for MeHg production as compared to additional Hg(II) inputs at Hg mining areas. Since the Hg safety of rice is the health guarantee for the global rice consumption population, our research results provide new insights into the accumulation of MeHg in paddy soil and the geochemical cycle of Hg species in paddy soil. The cycling pathways in natural environmental settings would be more complicated due to the dynamic nature of the ecosystems and influence from abiotic processes not accounted for here, i.e. light-driven Hg transformation. Still, our findings provide a useful stepping stone for rational management of rice paddy ecosystems to minimize Hg exposure and associated negative health effects.

CRediT authorship contribution statement

Qingqing Wu: Data curation, Formal analysis; Visualization, Writing original draft. **Baolin Wang:** Data curation, Methodology, Formal analysis, Writing review & editing. **Haiyan Hu:** Conceptualization, Funding acquisition, Supervision, Writing – review & editing. **Andrea G Bravo:** Formal analysis, Writing – review & editing. **Kevin Bishop:** Formal analysis, Writing – review & editing. **Stefan Bertilsson:** Formal analysis, Writing – review & editing. **Bo Meng:** Conceptualization, Funding acquisition, Supervision, Writing – review & editing. **Hua Zhang**: Funding acquisition, Supervision, Writing – review & editing. **Xinbin Feng:** Funding acquisition, Resources, Writing review & editing.

Declaration of Competing Interest

The authors declare that they have no known competing financial interests or personal relationships that could have appeared to influence the work reported in this paper.

Data availability

Data will be made available on request.

Acknowledgements

This work was supported by the National Natural Science Foundation of China (No. 41931297, 42273085, 42177114 and 41573078), the Guizhou Provincial Science and Technology Projects (ZK[2022]568), West Light Foundation of The Chinese Academy of Sciences, the Sino-Swedish Mercury Management Research Framework (SMaReF: VR2013-6978) and FORMAS (2016-00896). We thank Dr. Chenyan Ma at Beijing Synchrotron Radiation Facility (Beamline 4B7A) and Yu Song at Swedish University of Agricultural Science for assistance with the sulfur K-edge XANES spectroscopy measurements; Professor Alexandre J. Poulain from University of Ottawa for his suggestions and discussion in manuscript writing; Da Lei, Ruijie Sun and Qi Yang for their assistance in sample collection.

Appendix A. Supporting information

Supplementary data associated with this article can be found in the online version at doi:10.1016/j.jhazmat.2023.132486.

References

[1] Lindqvist, O., 1991. Special issue of first international on mercury as a global pollutant. Water Air Soil Pollut 56, 1-1.
[2] Mason, R.P., Reinfelder, J.R., Morel, F.M.M., 1996. Uptake, toxicity, and trophic transfer of mercury in a coastal diatom. Environ Sci Technol 30 (6), 1835–1845.
[3] Amin, S., et al., 2021. Mercury methylation and its accumulation in rice and paddy soil in degraded lands: A critical review. Environ Technol Innov 23, 101638.
[4] Su, Y.B., et al., 2016. Investigation of biogeochemical controls on the formation, uptake and accumulation of methylmercury in rice paddies in the vicinity of a coal-fired power plant and a municipal solid waste incinerator in Taiwan. Chemosphere 154, 375–384.
[5] Wang, Z.W., et al., 2019. Dimethylmercury in Floodwaters of mercury contaminated rice paddies. Environ Sci Technol 53 (16), 9453–9461.
[6] Feng, X.B., et al., 2008. Human exposure to methylmercury through rice intake in mercury mining areas, Guizhou Province, China. Environ Sci Technol 42 (1), 326–332.
[7] Liu, J.L., et al., 2012. Prediction of methyl mercury uptake by rice plants (Oryza sativa L.) using the diffusive gradient in thin films technique. Environ Sci Technol 46 (20), 11013–11020.
[8] Qiu, G.L., et al., 2005. Mercury and methylmercury in riparian soil, sediments, mine-waste calcines, and moss from abandoned Hg mines in east Guizhou province, southwestern China. Appl Geochem 20 (3), 627–638.
[9] Qiu, G.L., et al., 2008. Methylmercury accumulation in rice (Oryza sativa L.) grown at abandoned mercury mines in Guizhou, China. J Agric Food Chem 56 (7), 2465–2468.
[10] Meng, B., et al., 2011. The process of methylmercury accumulation in rice (Oryza sativa L.). Environ Sci Technol 45 (7), 2711–2717.
[11] Yin, R.S., Feng, X.B., Meng, B., 2013. Stable Hg isotope variation in rice plants (Oryza sativa L.) from the Wanshan Hg mining district, SW China. Environ Sci Technol 47 (5), 2238–2245.
[12] Wu, Q.Q., et al., 2020. Methanogenesis is an important process in controlling MeHg concentration in rice paddy soils affected by mining activities. Environ Sci Technol 54 (21), 13517–13526.
[13] Figueiredo, N., et al., 2018. Evidence of mercury methylation and demethylation by the estuarine microbial communities obtained in stable Hg isotope studies. Int J Environ Res Public Health 15 (10), 2141.
[14] Ramlal, P.S., et al., 1985. The effect of ph on methyl mercury production and decomposition in lake-sediments. Can J Fish Aquat Sci 42 (4), 685–692.
[15] Wang, J.X., et al., 2021. Mobilization, methylation, and demethylation of mercury in a paddy soil under systematic redox changes. Environ Sci Technol 55 (14), 10133–10141.
[16] Beckers, F., et al., 2019. Impact of biochar on mobilization, methylation, and ethylation of mercury under dynamic redox conditions in a contaminated floodplain soil. Environ Int 127, 276–290.
[17] Beckers, F., et al., 2019. Mobilization of mercury species under dynamic laboratory redox conditions in a contaminated floodplain soil as affected by biochar and sugar beet factory lime. Sci Total Environ 672, 604–617.
[18] Abdelhafiz, M.A., et al., 2023. DOM influences Hg methylation in paddy soils across a Hg contamination gradient. Environ Pollut 322, 121237.
[19] Graham, A.M., Aiken, G.R., Gilmour, C.C., 2013. Effect of dissolved organic matter source and character on microbial Hg methylation in Hg-S-DOM solutions. Environ Sci Technol 47 (11), 5746–5754.
[20] Gilmour, C.C., et al., 2013. Mercury methylation by novel microorganisms from new environments. Environ Sci Technol 47 (20), 11810–11820.
[21] Parks, J.M., et al., 2013. The genetic basis for bacterial mercury methylation. Science 339 (6125), 1332–1335.

[22] Benoit, J.M., Gilmour, C.C., Mason, R.P., 2001. The influence of sulfide on solid-phase mercury bioavailability for methylation by pure cultures of Desulfobulbus propionicus (1pr3). Environ Sci Technol 35 (1), 127–132.
[23] Benoit, J.M., et al., 1999. Sulfide controls on mercury speciation and bioavailability to methylating bacteria in sediment pore waters. Environ Sci Technol 33 (6), 951–957.
[24] Drott, A., et al., 2007. Importance of dissolved neutral mercury sulfides for methyl mercury production in contaminated sediments. Environ Sci Technol 41 (7), 2270–2276.
[25] Jonsson, S., et al., 2014. Differentiated availability of geochemical mercury pools controls methylmercury levels in estuarine sediment and biota. Nat Commun 5, 4624.
[26] Jonsson, S., et al., 2012. Mercury methylation rates for geochemically relevant HgII species in sediments. Environ Sci Technol 46 (21), 11653–11659.
[27] Schaefer, J.K., Morel, F.M.M., 2009. High methylation rates of mercury bound to cysteine by Geobacter sulfurreducens. Nat Geosci 2 (2), 123–126.
[28] Hu, H.Y., et al., 2013. Oxidation and methylation of dissolved elemental mercury by anaerobic bacteria. Nat Geosci 6 (9), 751–754.
[29] Bravo, A.G., et al., 2017. Molecular composition of organic matter controls methylmercury formation in boreal lakes. Nat Commun 8 (1), 14255.
[30] Gilmour, C.C., Henry, E.A., Mitchell, R., 1992. Sulfate stimulation of mercury methylation in freshwater sediments. Environ Sci Technol 26 (11), 2281–2287.
[31] King, J.K., et al., 2001. A Quantitative relationship that demonstrates mercury methylation rates in marine sediments are based on the community composition and activity of sulfate-reducing bacteria. Environ Sci Technol 35 (12), 2491–2496.
[32] Liu, Y.R., et al., 2019. Overlooked role of putative non-Hg methylators in predicting methylmercury production in paddy soils. Environ Sci Technol 53 (21), 12330–12338.
[33] Liu, Y.R., et al., 2018. Unraveling microbial communities associated with methylmercury production in paddy soils. Environ Sci Technol 52 (22), 13110–13118.
[34] Vishnivetskaya, T.A., et al., 2018. Microbial community structure with trends in methylation gene diversity and abundance in mercury-contaminated rice paddy soils in Guizhou, China. Environ Sci Process Impacts 20 (4), 673–685.
[35] Zhou, X.Q., et al., 2020. Microbial communities associated with methylmercury degradation in paddy soils. Environ Sci Technol 54 (13), 7952–7960.
[36] Hintelmann, H., Keppel-Jones, K., Evans, R., 2000. Constants of mercury methylation and demethylation rates in sediments and comparison of tracer and ambient mercury availability. Environ Toxicol Chem 19, 2204–2211.
[37] Barkay, T., Miller, S.M., Summers, A.O., 2003. Bacterial mercury resistance from atoms to ecosystems. FEMS Microbiol Rev 27 (2), 355–384.
[38] Barkay, T., et al., 1991. The relationships of Hg(II) volatilization from a freshwater pond to the abundance ofmer genes in the gene pool of the indigenous microbial community. Micro Ecol 21 (2), 151–161.
[39] Marvin-DiPasquale, M., et al., 2000. Methyl-mercury degradation pathways: A comparison among three mercury-impacted ecosystems. Environ Sci Technol 34 (23), 4908–4916.
[40] Ogunseitan, O., 1998. Protein method for investigating mercuric reductase gene expression in aquatic environments. Appl Environ Microbiol 64, 695–702.
[41] Siciliano, S.D., O'Driscoll, N.J., Lean, D.R.S., 2002. Microbial reduction and oxidation of mercury in freshwater lakes. Environ Sci Technol 36, 3064–3068.
[42] Schottel, J., et al., 1974. Volatilization of mercury and organomercurials determined by F factor system in enteric bacilli. Nature 251, 335–337.
[43] Schaefer, J., Letowski, J., Barkay, T., 2002. mer-Mediated resistance and volatilization of Hg(II) under anaerobic conditions. Geomicrobiol J 19 (1), 87–102.
[44] Bone, S.E., Bargar, J.R., Sposito, G., 2014. Mackinawite (FeS) reduces mercury(II) under sulfidic conditions. Environ Sci Technol 48 (18), 10681–10689.
[45] Gu, B.H., et al., 2011. Mercury reduction and complexation by natural organic matter in anoxic environments. Proc Natl Acad Sci USA 108 (4), 1479–1483.
[46] Jiang, T., et al., 2015. Modeling of the structure-specific kinetics of abiotic, dark reduction of Hg(II) complexed by O/N and S functional groups in humic acids while accounting for time-dependent structural rearrangement. Geochim Cosmochim Acta 154, 151–167.
[47] Barkay, T., Gu, B., 2022. Demethylation—the other side of the mercury methylation coin: A critical review. ACS Environ Au 2 (2), 77–97.
[48] Monperrus, M., et al., 2007. Mercury methylation, demethylation and reduction rates in coastal and marine surface waters of the Mediterranean Sea. Mar Chem 107 (1), 49–63.
[49] Wiatrowski, H.A., Ward, P.M., Barkay, T., 2006. Novel reduction of mercury(II) by mercury-sensitive dissimilatory metal reducing bacteria. Environ Sci Technol 40 (21), 6690–6696.
[50] Silver, S., Misra, T.K., 1984. Bacterial transformations of and resistances to heavy metals. Basic Life Sci 28, 23–46.
[51] Nazaret, S., et al., 1994. MerA gene-expression in aquatic environments measured by message-RNA production and Hg(II) volatilization. Appl Environ Microbiol 60 (11), 4059–4065.
[52] Poulain, A.J., et al., 2007. Potential for mercury reduction by microbes in the high arctic. Appl Environ Microbiol 73 (11), 3769-3769.
[53] Martin-Doimeadios, R.C., et al., 2004. Mercury methylation/demethylation and volatilization pathways in estuarine sediment slurries using species-specific enriched stable isotopes. Mar Chem 90 (1–4), 107–123.
[54] Spangler, W.J., et al., 1973. Methylmercury: bacterial degradation in lake sediments. Science 180 (4082), 192–193.
[55] Zhu, W., et al., 2018. Mercury transformations in resuspended contaminated sediment controlled by redox conditions, chemical speciation and sources of organic matter. Geochim Cosmochim Acta 220, 158–179.
[56] Zhao, L., et al., 2016. Mercury methylation in paddy soil: source and distribution of mercury species at a Hg mining area, Guizhou Province, China. Biogeosciences 13 (8), 2429–2440.
[57] Hu, H.Y., et al., 2020. Shifts in mercury methylation across a peatland chronosequence: From sulfate reduction to methanogenesis and syntrophy. J Hazard Mater 387, 121967.
[58] Zhao, L., et al., 2016. Mercury methylation in rice paddies and its possible controlling factors in the Hg mining area, Guizhou province, Southwest China. Environ Pollut 215, 1–9.
[59] Rodríguez Martín-Doimeadios, R.C., et al., 2002. Application of isotopically labeled methylmercury for isotope dilution analysis of biological samples using gas chromatography/ICPMS. Anal Chem 74 (11), 2505–2512.
[60] Gilmour, C.C., et al., 1998. Methylmercury concentrations and production rates across a trophic gradient in the northern Everglades. Biogeochemistry 40 (2), 327–345.
[61] Meng, B., et al., 2018. Tracing the uptake, transport, and fate of mercury in sawgrass (Cladium jamaicense) in the Florida Everglades using a Multi-isotope technique. Environ Sci Technol 52 (6), 3384–3391.
[62] Bravo, A.G., Loizeau, J.L., Dranguet, P., Makri, S., Bjorn, E., Ungureanu, V.G., et al., 2016. Persistent Hg contamination and occurrence of Hg-methylating transcript (hgcA) downstream of a chlor-alkali plant in the Olt River (Romania). Environ Sci Pollut Res 23, 10529–10541.
[63] Bustin, S.A., Benes, V., Garson, J.A., Hellemans, J., Huggett, J., Kubista, M., et al., 2009. The MIQE Guidelines: Minimum Information for Publication of Quantitative Real-Time PCR Experiments. Clin Chem 55, 611–622.
[64] Liang, L., Horvat, M., Cernichiari, E., Gelein, B., Balogh, S., 1996. Simple solvent extraction technique for elimination of matrix interferences in the determination of methylmercury in environmental and biological samples by ethylation gas chromatography cold vapor atomic fluorescence spectrometry. Talanta 43, 1883–1888.
[65] Song, Y., et al., 2020. Toward an internally consistent model for Hg(II) chemical speciation calculations in bacterium-natural organic matter-low molecular mass thiol systems. Environ Sci Technol 54 (13), 8094–8103.
[66] Cline, J.D., 1969. Spectrophotometric determination of hydrogen sulfide in natural waters. Limnol Oceano 13 (3), 454–458.
[67] Saywell, L.G., Cunningham, B.B., 1937. Determination of iron: Colorimetric o-phenanthroline method. Ind Eng Chem Anal Ed 9 (2), 67–69.
[68] Tjerngren, I., Karlsson, T., Bjorn, E., Skyllberg, U., 2012. Potential Hg methylation and MeHg demethylation rates related to the nutrient status of different boreal wetlands. Biogeochemistry 108, 335–350.
[69] Lehnherr, I., St Louis, Kirk, J.L., 2012. Methylmercury Cycling in High Arctic Wetland Ponds: Controls on Sedimentary Production. Environ Sci Technol 46, 10523–10531.
[70] Marvin-DiPasquale, M.C., Oremland, R.S., 1998. Bacterial methylmercury degradation in Florida Everglades Peat Sediment. Environ Sci Technol 32 (17), 2556–2563.
[71] Ravichandran, M., 2004. Interactions between mercury and dissolved organic matter—a review. Chemosphere 55 (3), 319–331.
[72] Du Laing, G., et al., 2009. Trace metal behaviour in estuarine and riverine floodplain soils and sediments: A review. Sci Total Environ 407 (13), 3972–3985.
[73] Liu, J., et al., 2022. The underappreciated role of natural organic matter bond Hg (II) and nanoparticulate HgS as substrates for methylation in paddy soils across a Hg concentration gradient. Environ Pollut 292, 118321.
[74] Colombo, M.J., et al., 2013. Anaerobic oxidation of Hg(0) and methylmercury formation by Desulfovibrio desulfuricans ND132. Geochim Cosmochim Acta 112, 166–177.
[75] Hu, H.Y., et al., 2013. Mercury Reduction and cell-surface adsorption by Geobacter sulfurreducens PCA. Environ Sci Technol 47 (19), 10922–10930.
[76] Lu, X., et al., 2016. Anaerobic mercury methylation and memethylation by Geobacter bemidjiensis Bem. Environ Sci Technol 50 (8), 4366–4373.
[77] Frohne, T., et al., 2012. Biogeochemical factors affecting mercury methylation rate in two contaminated floodplain soils. Biogeosciences 9 (1), 493–507.
[78] Oremland, R.S., Culbertson, C.W., Winfrey, M.R., 1991. Methylmercury Decomposition in sediments and bacterial cultures: Involvement of methanogens and sulfate reducers in oxidative demethylation. Appl Environ Microbiol 57 (1), 130–137.
[79] Hines, M.E., et al., 2012. Mercury methylation and demethylation in Hg-contaminated lagoon sediments (Marano and Grado Lagoon, Italy). Estuar Coast Shelf Sci 113, 85–95.
[80] Hines, M.E., et al., 2000. Mercury biogeochemistry in the Idrija River, Slovenia, from above the mine into the Gulf of Trieste. Environ Res 83 (2), 129–139.
[81] Baldi, F., Pepi, M., Filippelli, M., 1993. Methylmercury resistance in Desulfovibrio desulfuricans strains in relation to methylmercury fegradation. Appl Environ Microbiol 59 (8), 2479–2485.
[82] Jonsson, S., Mazrui, N.M., Mason, R.P., 2016. Dimethylmercury formation Mediated by inorganic and organic reduced sulfur surfaces. Sci Rep 6 (1), 27958.
[83] Asaduzzaman, A.M., et al., 2010. Computational studies of structural, electronic, spectroscopic, and thermodynamic properties of methylmercury-amino acid complexes and their Se analogues. Inorg Chem 49 (3), 870–878.
[84] Khan, M.A.K., Wang, F., 2010. Chemical demethylation of methylmercury by selenoamino acids. Chem Res Toxicol 23 (7), 1202–1206.

[85] Lindqvist, O., et al., 1991. Mercury in the Swedish environment — Recent research on causes, consequences and corrective methods. Water Air Soil Pollut 55 (1) xi-261.
[86] Liu, J., et al., 2021. Stable isotope tracers identify sources and transformations of mercury in rice (Oryza sativa L.) growing in a mercury mining area. Fundam Res 1 (3), 259–268.
[87] Beckers, F., Rinklebe, J., 2017. Cycling of mercury in the environment: sources, fate, and human health implications: a review. Crit Rev Environ Sci Technol 47 (9), 693–794.